Corrosion and Tribocorrosion Performance of pack carburized Commercially Pure Titanium with Limited Oxygen diffusion in a 0.9% NaCl Solution.

R. Bailey*, Y. Sun

School of Engineering and Sustainable Development
Faculty of Technology
De Montfort University
Leicester, UK

Corresponding author- email: Richard.bailey@dmu.ac.uk

Abstract

In the research presented, the corrosion and tribocorrosion characteristics of pack carburized titanium with limited oxygen diffusion (PCOD-Ti) has been investigated using a 0.9 % NaCl solution. The carburization treatment was undertaken using a service temperature of 925 ℃ for duration of 20 h. The treatment resulted in the creation of a titanium carbide (TiC) network layer atop an extended oxygen diffusion zone (ODZ) (α-Ti(O)). Electrochemical testing indicated the treated titanium surface offered slightly enhanced corrosion resistance over that of untreated titanium. Tribocorrosion testing of the PCOD-Ti was conducted by sliding the titanium against an alumina counter-face under a contact load of 20 N, with various anodic and cathodic potentials applied. The testing showed a dramatic reduction in the wear rate for the treated titanium. Wear rates were reduced by an order of magnitude when compared with the untreated samples. During testing an interesting cathodic protection was encountered. When subjected to high negative charge the wear rates of the treated titanium were reduced further. This reduced wear was attributed to the formation of titanium hydride within the wear track.

Word Count: 179

Keywords: Titanium, Carburization, Corrosion, Tribocorrosion and Wear

1. Introduction

Titanium processes low density, high strength and excellent corrosion resistance [1,2]. These key properties have allowed titanium to be used in many industrial sectors, some of the key industries where titanium has been utilized include the aerospace and biomedical sectors [3]. Titanium has found particular importance in the biomedical sector due to its excellent biocompatibility [4,5]. Compared to other orthopaedic implant materials titanium is seen as the best match to cortical bone. Table 1 shows various bio-metals and how their key properties compare with that of bone. The data shows titanium to have the lowest elastic modulus, although not a true match to bone, it is by some way the best choice. Titanium also has an advantage over the other metals due to its excellent strength to weight ratio, these properties have enabled extensive use in dental implants [6,7], intramedullary nails [8] and femoral stems [9]. However, so far the uses of titanium have been restricted to non tribological components/structures [10,11]. Titanium has a well-known tendency to seize and suffer from severe galling when subjected to sliding surface contact [12,13].

To improve the tribological response of titanium, various surface treatment techniques have been developed, these include: Boronizing [14], Nitriding [10], Oxidation [15,16] and carburization [17-19]. These techniques aim to modify the surface for low friction and wear, while maintaining the bulk characteristics of the titanium. These treatments to date only offer improved performance when the components are subjected to relatively low contact loads. When the contact loads are increased the coatings do not provide sufficient protection [20].

To improve the load bearing capacity of titanium a new surface treatment technique has been developed. Pack carburization with limited oxygen diffusion (PCOD) has been shown to greatly reduce wear and offer a low coefficient of friction when in dry conditions under very high contact pressures (1GPa) [21]. The PCOD-Ti process produces a hard (2000 HV) titanium carbide/oxycarbide network layer atop an extended oxygen diffusion zone (α-Ti(O)). So far testing of this new treatment has been confined to dry sliding conditions [21]. It is also interesting to note that recent studies into the osseointegration of TiC [22,23], have shown TiC can greatly improve the osseointegration of titanium implants. The *in vitro* and *in Vivo* tests conducted showed the TiC coated implants achieved increased biocompatibility by stimulating osteoblast proliferation and adhesion activity.

This present work aims to understand the corrosion and tribocorrosion behavior of titanium that has been treated using the PCOD process. During the investigation the variation in corrosion response relative to the surface depth was characterized by mechanically

removing surface layers across the carburized titanium. This method builds up a picture of the samples corrosion characteristics as a function of depth, helping to understand the electrochemical state of the material during tribocorrosion testing. The tribocorrosion characteristics of the coating were then investigated. The contribution of both mechanical abrasion and electrochemical wear were analyzed by controlling the surface potential. All results are reported and discussed in this paper.

Table 1: The material properties of cortical bone and some of the commonly used biomaterials [24] [24].

Material	**CTE (μstrain/°C)**	**Density (kg/m^3)**	**Elastic modulus (GPa)**	**Tensile strength (MPa)**
Ti (grade 2)	8.75	4515	102.5	417.5
St. Steel (AISI 316LVM)	16.5	7990	187.5	590
Co-Cr (CCM)	12.8	8290	241	968
Bone (air dry)	20	1950	19.5	140

2. Experimental

2.1. Sample preparation and Characterization

The substrate material used during this study was that of commercially pure, grade 2 titanium (CP-Ti), with a composition of: Ti/<0.1 C/<0.3 Fe/<0.015 H/<0.03 N/<0.25, by percentage weight. All samples during this study were cut from a 2 mm thick plate and then progressively ground with SiC grinding pads to a grit of P1200. This resulted in a surface finish of 0.2 µm (R_a). The samples were then ultrasonically cleaned in methanol for 15 min to remove grinding particles.

The samples were then treated using a pack carburization process with limited oxygen diffusion (PCOD). The treatment was undertaken using a St Steel container with an internal volume of 200 cm^3 of which 140 cm^3 was filled with carburizing compound, as shown in Fig.1. A previous study[21] showed an effective carburizing compound should consist of: Carbon (C), Barium carbonate ($BaCO_3$), Calcium carbonate ($CaCO_3$) and Sodium carbonate ($NaCO_3$) in a ratio of 6:3:2:1 respectively. The samples were then heated to 925 ℃ for 20 h and allowed to furnace cool to room temperature. These parameters have previously been shown to generate a network like carbon rich structure with uniformity to a depth of ≈7 µm. Fig.2a shows the cross sectional structure produced by the carburization process. Fig.3 shows an SEM image of the network like structure generated at the surface of the treated titanium. The Oxygen and carbon concentration profiles as a function of depth were collected using glow discharge optical spectroscopy (GDOS) and can be seen in Fig.2b. These plots show how the carbon concentration is high at the surface to a depth of ≈ 15 µm and then drops off, while the oxygen concentration remains stable. X-ray diffraction patterns (See Fig.4) have shown this network structure to consist mainly of titanium carbide and sits atop a ≈ 200 µm deep ODZ [21]. After treatment the samples were lightly polished to remove any pack residue attached to the samples surface. The samples were then ultrasonically cleaned in methanol for 15 min.

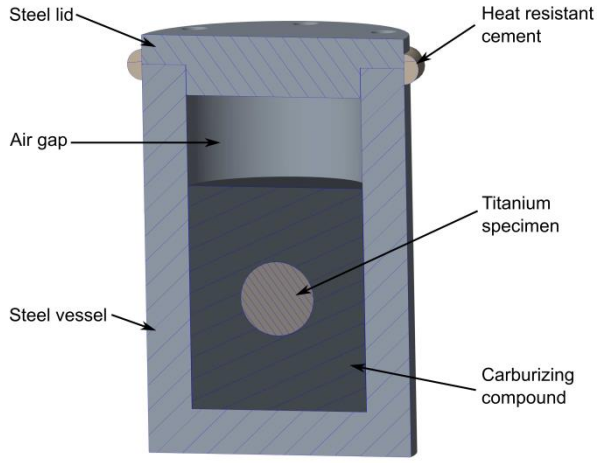

Fig.1: 3D render of the carburizing container.

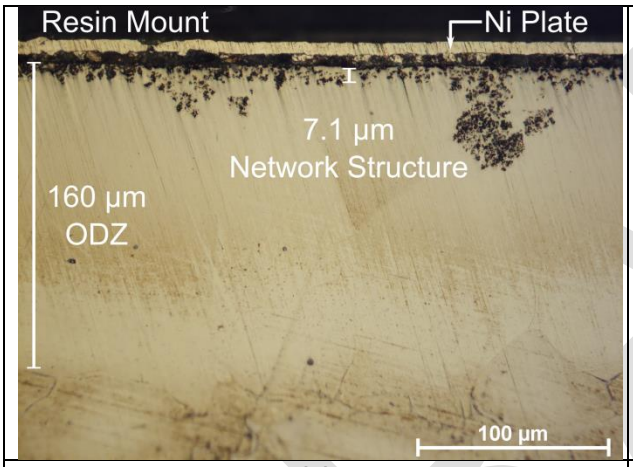

(a)

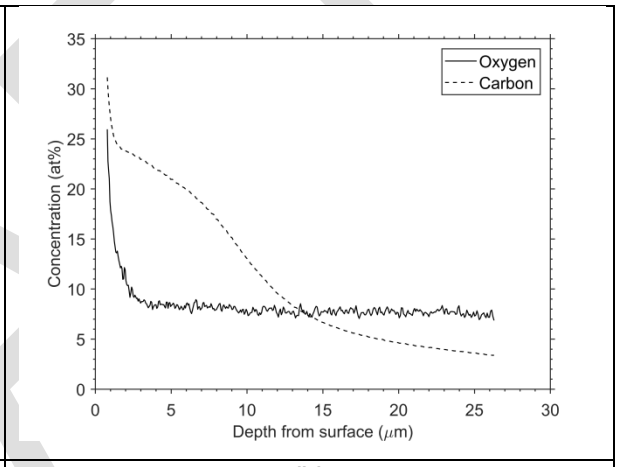

(b)

Fig.2: (a) Optical image showing the etched cross sectional structure of the pack carburized titanium and (b) Carbon and oxygen concentration profiles measured by GDOS across the TiC network produced at 925 ℃ for 20 h on CP-Ti.

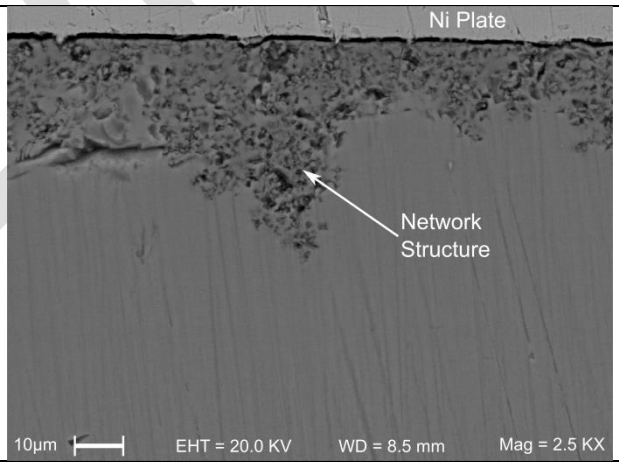

Fig.3: SEM image showing the TiC network layer in detail.

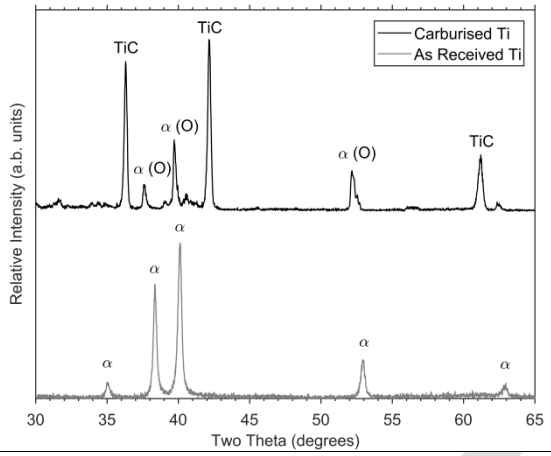

Fig.4: XRD patterns generated from the PCOD-Ti.

2.2. Electrochemical corrosion tests

Electrochemical corrosion tests were performed using a Princeton applied research model K0235 three-electrode electrochemical flat cell connected to an ACM Gill AC potentiostat equipped with a data logger. The specimen was clamped to the cell, which exposes 1.0 cm^2 of the specimen surface to the electrolyte. A schematic of this setup is shown in Fig. 5. The reference electrode was a saturated calomel electrode (SCE), with all potentials referring to the SCE scale. The electrolyte used for all tests was 0.9 % NaCl solution, which was prepared from analytical grade chemicals and distilled water. All tests were performed at standard room temperature (20 °C) open to the air.
The 0.9% NaCl (saline) solution was used to perform baseline tests, many studies have used this medium as the first port of call for understanding the response of coated biomedical metals [Topan-2017, Doni-2013, Barril-2005 and Liu-2004]. The saline solution replicates the salinity found in the human body and is tribologically conservative by neglecting the friction lowering properties offered by saline-bovine serum solutions [YS-2017].
After an initial surface test, progressive grinding of the pack carburized titanium was undertaken using 1200P SiC Paper. Progressive grinding was used to expose the underlying structure at various depths from the surface. 2-3 µm of material was removed with each stage of grinding, this was measured using a digital micrometer accurate to 1 µm. After cleaning ultrasonically in methanol for 300 s, the samples were then loaded into the electrochemical test cell and then catholically charged at -500 mV for 180 s to create a uniformed starting point for all samples. Each exposed layer was then tested using the following electrochemical techniques.
Potentiodynamic polarization measurement was performed using a sweep rate of 1 mVs^{-1}, starting from a cathodic potential of -400 mV_{SCE} (vs. open circuit potential (OCP)), then to an anodic potential of 1500 mV_{SCE} (vs. OCP).
Current transient measurements were performed by potentiostatically polarizing the specimens at a constant potential of 500 mV_{SCE} for 3600 s. The variation in current density with time was recorded continuously throughout the test.

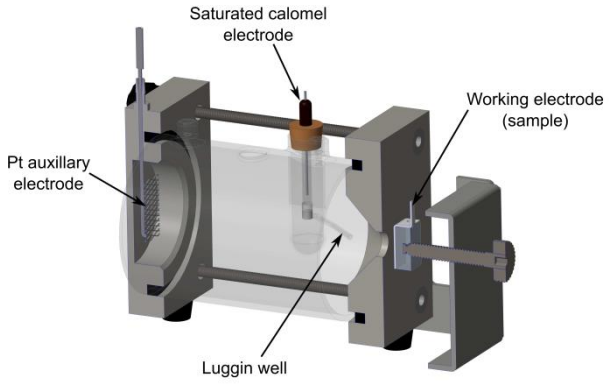

Fig.5: 3D renders of the electrochemical cell used in this study.

2.3. Tribocorrosion tests

Tribocorrosion tests were conducted using a Teer Coatings pin on disk tribometer which has been modified to incorporate an electrochemical cell through the addition of electrodes and a nylon sample holder, as shown in Fig. 6. During testing the sample area exposed to the electrolyte was controlled to 1.23 mm^2 using lacquer. During the tests the tribometer was set to rotate at a speed of 60 rpm with a track diameter of 9 mm, this represents a sliding speed of 2.8 cm/s. The pin material and geometry was that of an 8 mm diameter Alumina Ball (manufactured by Trafalgar bearings), a load of 20 N was applied to the sample through the Alumina ball. Alumina was chosen as it is hard (1600 HV [24]) and inert. The inert nature of the alumina removes the interaction of the counter material with the test electrolyte.

During this study all tests were conducted in a 0.9 % NaCl solution at room temperature (20 ℃) and pressure. Once the samples were emerged into the electrolyte a stabilization period was initiated. This period lasted 30 min, during this time the test cell was rotated with no surface contact. After the initial stabilization period the contact was engaged for a duration of 4 hours, this equates to a sliding distance of ≈ 408 m. After the 4 hours of sliding contact another 30 min of material stabilization was conducted. During the tribocorrosion tests the samples were potentiostatically polarized at potentials of +1000, +500, -900 and -1500 mV_{SCE}, OCP measurements were also taken.

Wear rates were evaluated using the wear track profiles generated during the sliding contact. Using A mitutoyo SJ-400 stylus type profilometer the wear track profile was measured in 8 locations. The wear track volume was then estimated. Using the wear track volume (V), the applied load (L) and the sliding distance (S_d) then the total material loss rate (TMLR) can be calculated from Eq.1.

$$TMLR = \frac{V}{d_s \times L} \quad (1)$$

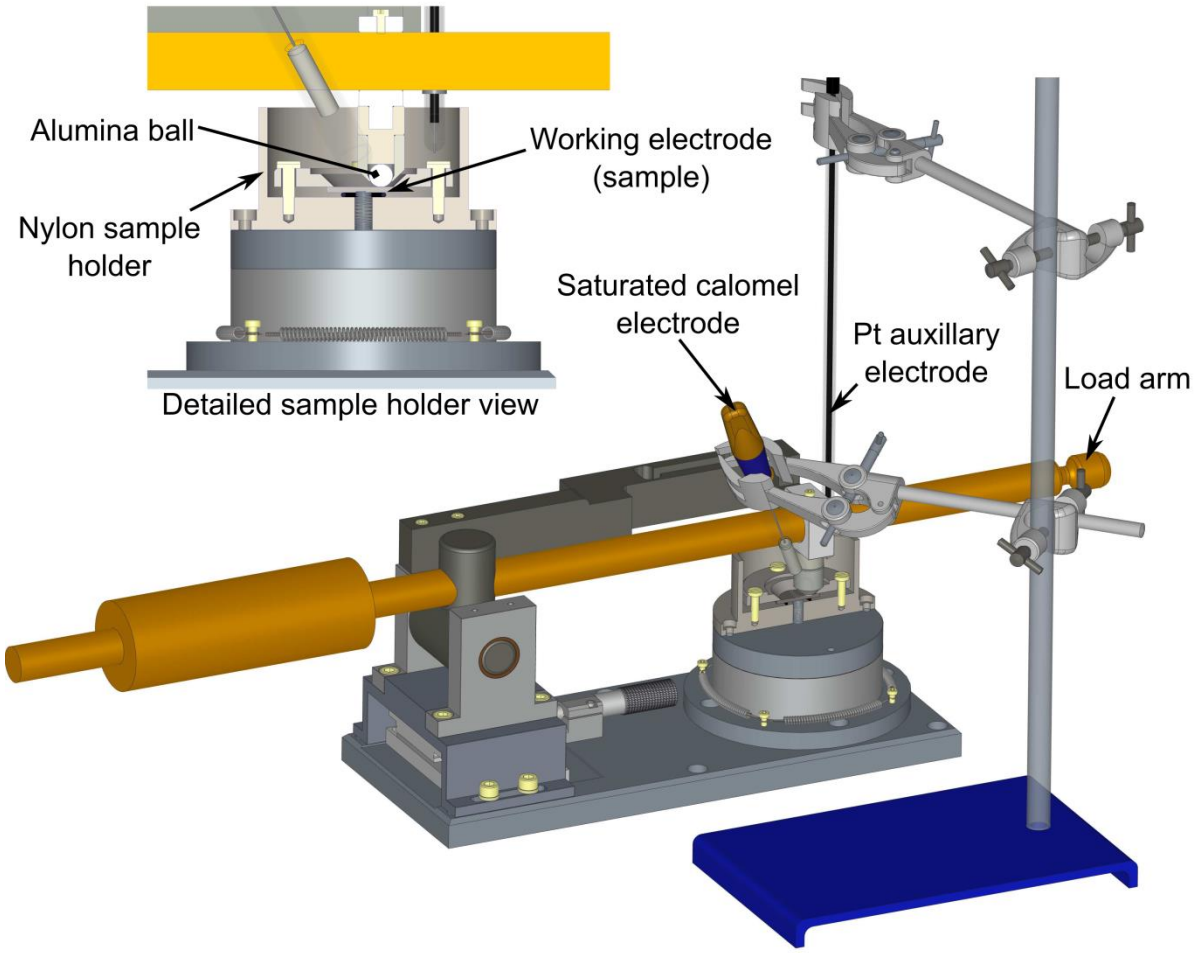

Fig.6: 3D renders of the tribocorrosion test apparatus.

3. Results and discussion

3.1. Electrochemical behaviour as a function of depth from the carburized surface

3.1.1. Potentiodynamic behaviour

Fig. 7 shows potentiodynamic polarisation curves for the PCOD-Ti at various depths from the as-carburised surface, correlating to different amounts of carbon and oxygen within the substructure. The polarisation curves show that the carbon rich surface layer results in an anodic shift in the free corrosion potential to -200 mV_{SCE} from approximately -500 mV_{SCE} for untreated CP-Ti. However, the welcomed shift in corrosion potential comes with higher current densities throughout the potential sweep. Both the anodic shift and current densities have been reported previously [25]. Oláh et al found that TiC coatings have an improved corrosion potential but suffer from a greater rate of corrosion. The density of the TiC film was given as the attributing factor toward the increased corrosion rate. Thinner less dense TiC films would have a greater porosity and a higher defect density.

Using the PCOD technique, allows for the surface film generated to consist of multiple titanium, carbon and oxygen phases, these phases include: TiC, TiO_2, TiO, TiC_xO_{1-x} and α-Ti. XRD (Fig. 4) demonstrated that TiC is mostly formed at the surface but other stoichiometry cannot be ruled out. The Pourbaix diagram of TiC (Fig.8), shows that when exposed to a neutral solution (0.9 % NaCl, pH ≈ 7) a titanium dioxide (TiO_2) boundary layer will be formed along with methane (CH_4) this was also demonstrated by [26]. Considering this, overall the rate of TiO_2 formation during corrosion will vary depending on the film composition at any one point. This will lead to a film of varying density and porosity, resulting in an increased rate of dissolution as seen during the anodic sweep. The carbon rich region persists with consistent polarisation sweeps to a depth of around 10 µm this is consistent with the carbon concentration profile produced via GDOS (Fig.2b).

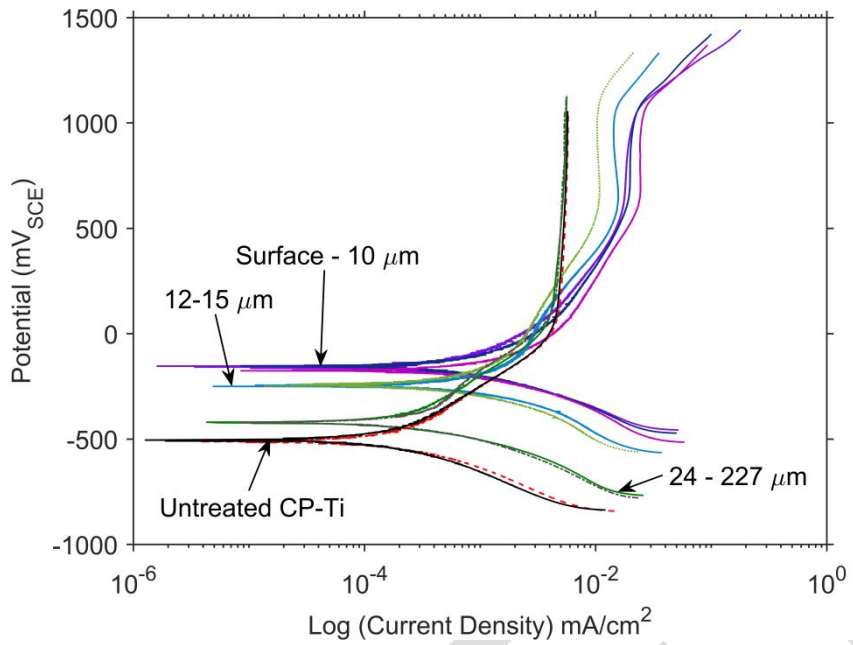

Fig.7: Anodic polarisation curves measured for PCOD-Ti at various depths from the treated surface, using a sweep rate of 1 mVs^{-1} in a 0.9 % NaCl solution.

There is then a transitional period where the anodic shift is less pronounced and the anodic corrosion currents are reduced, this period seems linked to the amount of carbon in the substructure. Once the surface was ground to a depth of 24 µm, the polarisation curves show consistency to a depth of around 230 µm from the surface. This zone is within the observed ODZ. There is a slight anodic shift in the free corrosion potential 400 mV$_{SCE}$ compared with that of untreated titanium (-500 mV$_{SCE}$). In this range there is reduced current density compared to the surface in the anodic region and are similar to those of untreated titanium. This response of oxygen rich titanium has been observed in the thermally oxidized titanium [16]. Oxygen in the diffusion zone seems to have a slight positive effect on the corrosion properties of titanium by creating a higher corrosion potential (-400 mV$_{SCE}$). At further depths (290 µm and deeper) from the surface, the oxygen content is much reduced and the material's electrochemical response shows a very reproducible and consistent polarisation curve with a stable passive region between 200 mV$_{SCE}$ and 1000 mV$_{SCE}$, where current density is stable at around 0.005 mAcm^{-2}, which is similar to that of untreated CP-Ti.

It seems that the PCOD process allows for a large anodic shift in the corrosion potential meaning that initially it will be quite resistant to corrosion, however when corrosion starts the carburised titanium will dissociate at a slightly faster rate than untreated titanium.

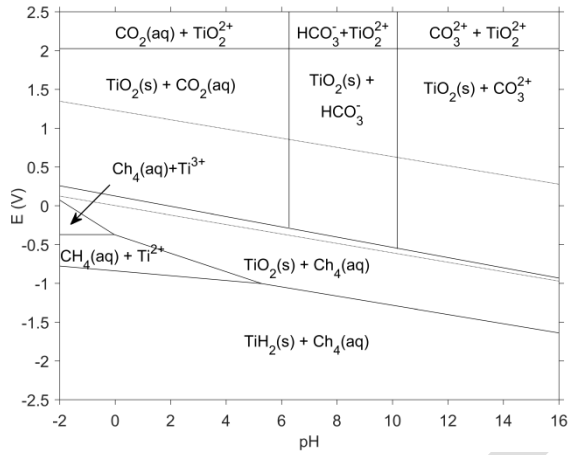

Fig.8: Pourbaix diagram for titanium carbide (E/pH).

3.1.2. Current transient behavior

Potentiostatic testing was carried out at various sample depths by applying a potential of 500 mV_{SCE} for 3600 s. According to Fig.7, at this potential all samples are within the passive region. The Pourbaix diagram for titanium carbide (Fig.8) also shows that when polarised at 500 mV_{SCE} in a neutral pH solution, a TiO_2 surface film should be generated. Fig.3 shows the current transient response for the samples in the Log (I) vs. Log (t) scale. Using the point defect model and the high field theory the current response over time is described by Eq.2. A plot of Log (I) and Log (t) should produce a straight line. For a dense adherent film the gradient (k) should equal 1, for less dens films the gradient will be less [27-29].

$$I = 10^{[-A+\mathrm{klog}(t)]} \quad (2)$$

In Fig.9 the curves generated for the ground samples clearly conforms to Eq.2. There exists an initial stage in all the tested samples where there are lower curve gradients (≈0.5). This low value of k is attributed to small film thickness in the initial stage of polarisation, a phenomenon that has been reported in previous studies [27,28]. As polarisation time increases the passive film thickens and the k value approaches 1. Once again, it can be observed that there is a variation between the current densities observed in the carbon rich region and the oxygen rich region below.

From the surface until a depth of 10 µm the curve reaches linearity sooner after around 10 s this is much faster than at deeper depths (≈ 200 s). This carbon rich zone never reaches k = 1. The upper diffusion zone with high oxygen content also never achieves this ideal value for k. Whereas, the further ground samples all achieve this ideal value as expected for titanium [16]. This variation in the time to reach the linear stage and final slope value shows that when there is a high carbon and oxygen content present within the titanium lattice, a passive film can be formed very quickly, this results initially in lower current density. This faster response could be attributed to the higher free corrosion potential observed in Fig.7. However, with larger carbon and oxygen content present the data in Fig.9 suggests that the film generated is less dense and more porous than that produced when lower carbon concentrations are present within the titanium structure.

The ODZ reaches linearity in around 10 s but initially there is higher current density when compared with the carbon rich zone. A previous study [30] investigating thermally oxidised titanium showed the ODZ to have similar characteristics, the film was fast forming but, had a lower than ideal k value. Using Mott-Stocky the study demonstrated that the ODZ had a higher defect density than that of untreated titanium or titanium with lower oxygen content. Therefore, PCOD-Ti will undoubtedly have a high defect density in the close to medium sub surface (0 – 100 µm). Increased levels of carbon and oxygen result in various titanium phases present at any one time, these phases include: TiC, TiO_2, TiO, TiC_xO1_{-x} and α-Ti etc… With all these varying phases, galvanic corrosion can occur. With multiple phases present, local cells can develop, resulting in a faster dissociation [31]. The incorporation of carbon within TiO_2 will also generate extra interstitial sites, this will allow for greater

ion transportation. This would explain the increases corrosion current observed during anodic potentials in the carbon rich near surface region, see Fig.7.

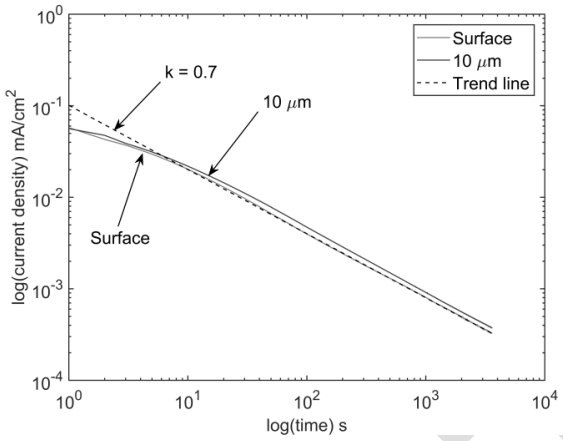

(a)

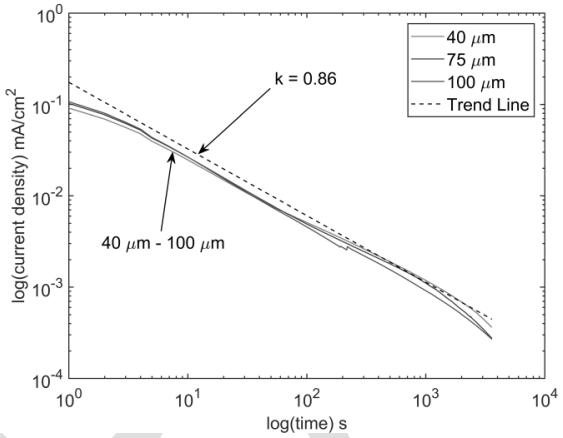

(b)

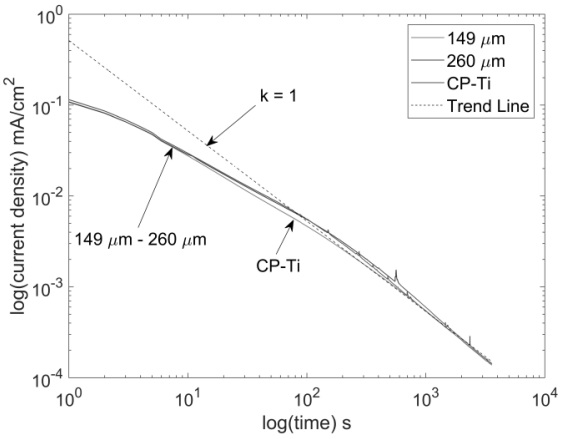

(c)

Fig.9: Current transient curves in the log (I) vs. log(t) scale measured during film formation at various depths from the surface of pack carburised titanium with (a) showing the carbon rich surface layers, (b) shows the Oxygen rich diffusion zone and (c) shows the lower ODZ and untreated titanium. All tests were conducted at a potential of 500 mV for duration of 3600 s in a 0.9 % NaCl solution.

3.2. Tribocorrsion behavior

3.2.1. Open circuit Tribocorrosion behavior

Initial tribocorrosion tests were carried out in an open circuit without externally applied potential. The samples were tested for a duration of 3 h with 2 h sliding with 30 min stabilisation before and after sliding. Fig.10 shows the evolution of potential and friction coefficient over time for the PCOD-Ti samples. During tribocorrosion testing, three distinct frictional zones are observed, these friction zones were also observed during dry sliding [21].

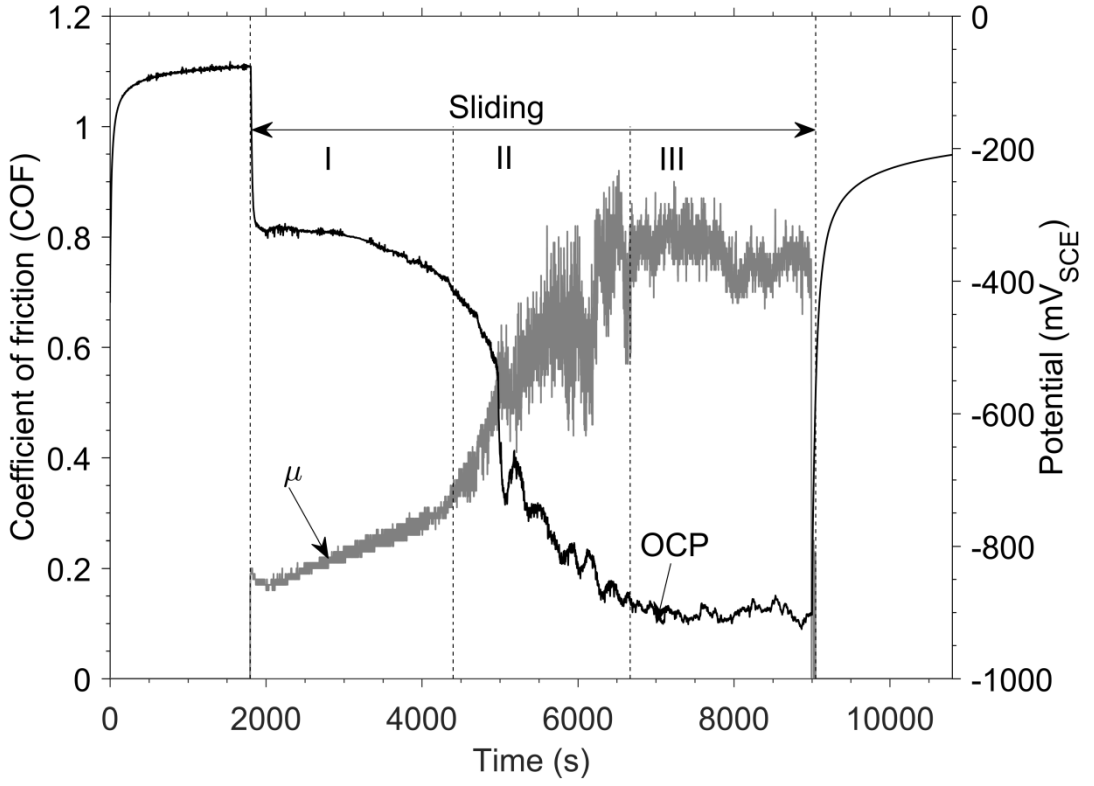

Fig.10: Open circuit potential and Coefficient of friction curves recorded for a contact load of 20 N in a 0.9 % NaCl solution for PCOD-Ti. The onset of sliding is indicated after 30 minutes stabilisation. Four distinct frictional zones can be observed: I) Oxide layer, II) Partial removal of the oxide layer and III) Oxygen diffusion zone.

It is proposed that each zone observed is related to the materials composition and substructure. The PCOD treatment generates a multilayer structure within the Ti. The frictional response over time is dependent on the structure and the transition between each layer as wear progresses. The friction zones observed in Fig. 10 relate to the following structural transitions: (I) carbide layer, (II) the removal of the carbide network and (III) the ODZ. Zone IV characterised by the exposure of Ti substrate, identified in [16], would have been observed had the test run for a longer duration. With the identification of the three frictional zones, it can clearly be seen that the OCP plot also correlates with these frictional zones.

OCP gives insight into the surface condition of the samples in real time during the sliding wear process. Each zone exhibits a unique friction and OCP response correlating to the varying levels of material activity:

Zone I: Sliding contact between the Al_2O_3 ball and the carbide network layer results in low friction. The OCP plot shows an initial cathodic shift from -100 mV to -300 mV. As the carbide layer is worn the potential gradually drops from -300 mV to -400 mV, during this time the friction coefficient gradually rises from 0.2 to 0.3 over a time period of 3200 s.
Zone II: As the sliding continues, the carbide network layer is gradually removed or damaged, exposing the ODZ. This transitional period results in a cathodic drop in potential from -400 mV to -900 mV. This drop in OCP coincides with a dramatic increase in friction coefficient form 0.3 to 0.8 in just 2100 s.
Zone III: Full exposure of the ODZ to the contact zones results in a stabilisation in the OCP (≈ -900 mV) and friction ($\mu \approx 0.8$)

When considering the tribocorrosion response of PCOD-Ti, it is interesting to compare the frictional response in both the corrosive medium (0.9 % NaCl in Fig. 4) and in a dry un-lubricated medium. A previous study [21] has been conducted looking at the dry sliding of PCOD-Ti against and Al_2O_3 ball with a contact load of 20 N. During the present study the TiC network layer was able to withstand the load for 10800 s (3 h), all while producing a low coefficient of friction. However, during this study with the same load in a 0.9 % NaCl solution the low friction was observed for just 3200 s (< 1 h) This reduced level of protection is clearly generated by the interaction between the surface carbide and the corrosive medium.

Avgustinik et al. showed that titanium carbide is decomposed by water at room temperature to form TiO_2 to a depth of 1500 Å from the surface by the reaction described in Eq.3.

$$TiC + xH_2O \rightarrow TiO_2 + CH_4 + xH_2O \quad \textbf{(3)}$$

Therefore, during wear the sliding contact will be between TiO_2 and the Al_2O_3 slider. The subsequent removal and reformation of the TiO_2 layer can be accredited to the increased wear rate observed when in a corrosive medium.

3.2.2. The effect of applied potential on the Tribocorrosion behavior

In order to understand the contributing factor of corrosion on the overall tribocorrosion behaviour of PCOD-Ti, potentiostatic sliding wear tests were performed at both anodic and cathodic potentials of +1000, +500, -900 and -1500 mV_{SCE}. Fig.10 shows both the friction and current traces recorded at each potential, it is clear that the applied potential has a significant impact on the frictional response of the PCOD-Ti.

At anodic potentials accelerated corrosion is usually expected as this favours the anodic forward reaction. Fig. 10.a and 10.b show the friction and the current for the samples polarised at 1000 mV_{SCE} and 500 mV_{SCE} respectively. The frictional response of both samples is very similar with low friction ($\mu < 0.4$) observed throughout the test. The current flow is clearly affected by the onset of sliding; when sliding is initiated there is a sharp jump in the measured current density showing an activation of the surface. The amount of current flow is proportional to the applied potential, the higher the potential the higher the current. This is as expected, when polarised in the anodic region we are actively encouraging corrosion to take place and this higher the potential the greater the rate of dissociation.

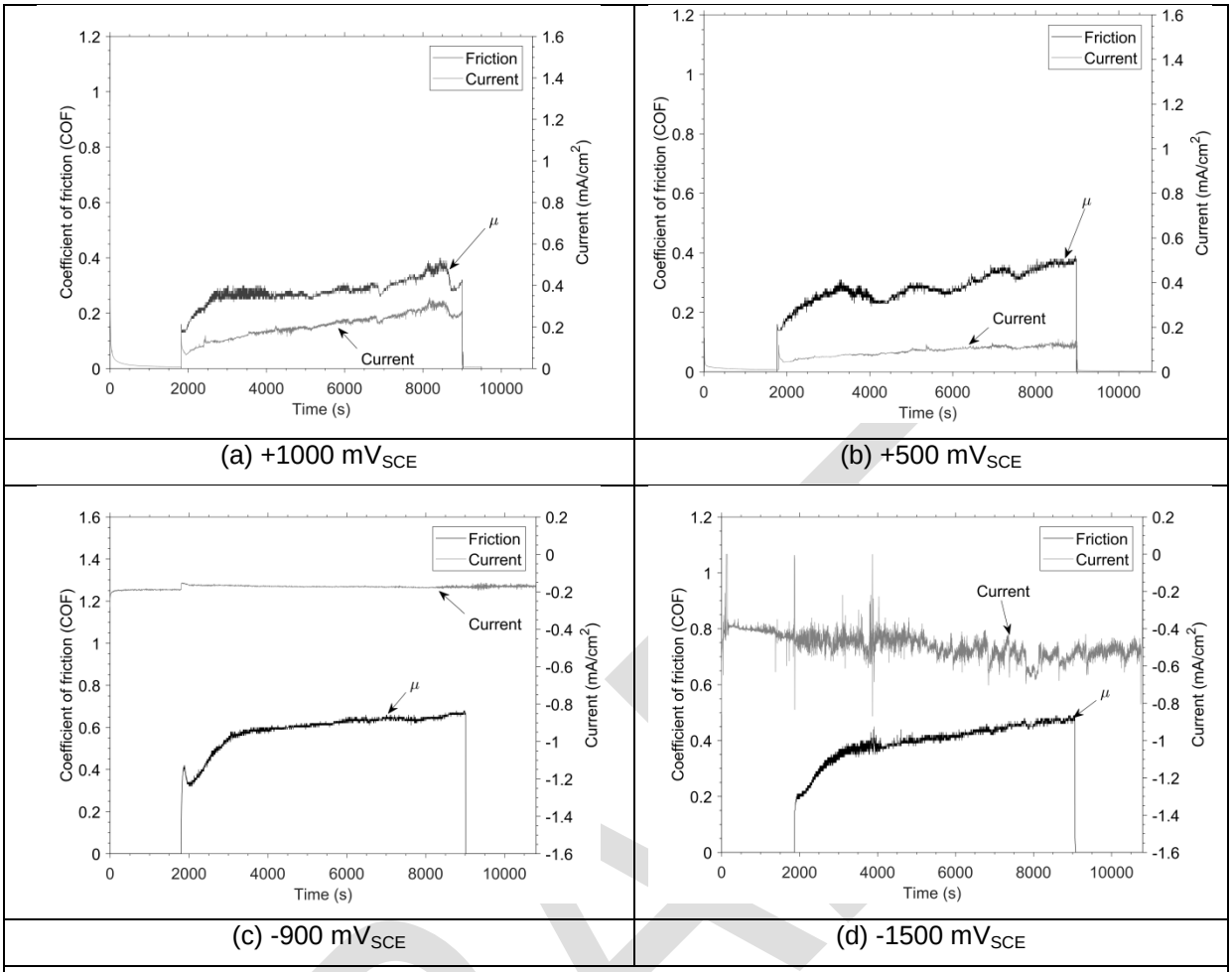

(a) +1000 mV_{SCE} (b) +500 mV_{SCE}

(c) -900 mV_{SCE} (d) -1500 mV_{SCE}

Fig.10: Friction coefficient (μ) and current density (I) against time for tribocorrosion testing at potentials of: (a) 1000 mV_{SCE}, (b) 500 mV_{SCE}, (c)-900 mV_{SCE} and (d) -1500 mV_{SCE}.

When we consider the frictional response of these samples it is important to make comparisons to that of the samples tested at OCP (Fig.9) in order to understand how corrosion affects the wear mechanisms. When PCOD-Ti is anodically charged the samples no longer display the three frictional zones highlighted under OCP conditions. These differences are also evident when looking at the wear track morphology produced after sliding for the 1000 mV_{SCE} (Fig.11.a), 500 mV_{SCE} (Fig.11.b) and the OCP sample (Fig.11.c), there is a clear shift in wear mechanism from that at OCP and anodic potentials. Wear track morphology of the samples tested at OCP show exposure of the underlying ODZ within the centre of the wear tracks with large amounts of adhesive wear observable, this is also highlighted by the large coefficient of friction recorded in Fig.9. The wear tracks also reveal wear through the carbide layer proceeds via simple abrasive polishing highlighted by the smooth appearance of the wear track. Over time small cracks generate, these then propagate and result in de-lamination, this is classic fatigue. The anodically charged samples were tested under the same load and duration as the OCP samples. However, throughout the duration the test the coefficient of friction never surpassed 0.4. When looking at the wear track morphology of these samples the dominating wear mechanism is that of simple abrasion with a very smooth wear track and large scale de-lamination. On closer inspection there are areas where some delamination has occurred through

the creation and propagation of micro cracks within the wear track, this is more evident in the 500 mV_{SCE} (Fig.11.b) sample.

This change in wear mechanism can be attributed to the formation of a TiO_2 layer at the samples surface via the decomposition of TiC [26]. At anodic potentials Eq.3 can penetrate to depths much greater than 150 Å and produce a protective layer that will not be fully removed with each subsequent pass of the slider. This constant film removal and formation within the wear track would result in the smooth polished like surface observed. This would also account for the low friction coefficients observed due to the enhanced tribological properties of TiO_2.

When a metal is cathodically charged it is possible to remove the corrosive element of wear during the tribocorrosion process. By applying a negative charge to the sample it is no longer possible to generate the metal cations (M^+) required for corrosion. However, when the polarisation is taken to the extreme negative potentials, hydrogen production can occur at the samples surface via the electrolysis of water. This can result in hydrogen uptake by the cathode material, this is known as hydrogen embitterment [32-36]. When PCOD-Ti was cathodically charged to -900 mV_{SCE} and -1500 mV_{SCE} the frictional response was very different form that encountered at OCP (see Fig.10.c and 10.d respectively). Again the frictional response was no longer characterised by three distinct zones, when polarised to -900 mV_{SCE} the friction gradually reached 0.6 at which it then stabilised and the -1500 mV_{SCE} sample reached a stable friction coefficient of 0.4. This strange frictional response could be attributed to hydrogen embitterment and the formation of TiH_2.

SEM wear track images for the -1500 mV_{SCE} (Fig.11.e) and -900 mV_{SCE} (Fig.11.d) samples show the formation of a surface layer within the wear track, typified by a smooth polished appearance with large scale cracking and delamination. It would seem the amount of hydrogen present within the wear track is directly related to the frictional response of the samples. The samples tested at -1500 mV_{SCE} would have a greater hydrogen uptake than that treated at -900 mV. This should explain the difference in frictional response between the two samples. The sample treated at -1500 mV_{SCE} would have a much more uniformed covering of TiH_2, compared with -900 mV_{SCE} which is much more likely to have a mixed phase surface consisting of TiH_2, TiH, TiC, TiO_2, TiO, Ti, and any intermediate phases, this could result in increased friction due to the uneven wear of each phase.

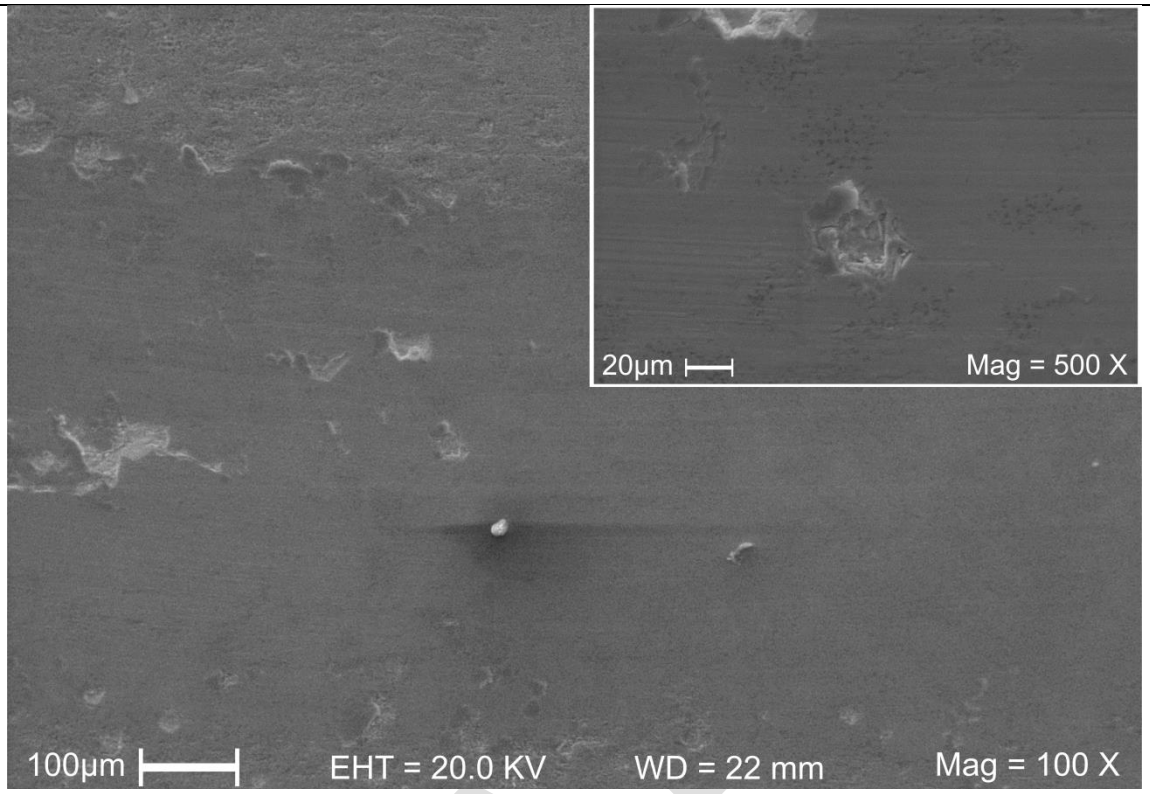

(a) +1000 mV_{SCE}

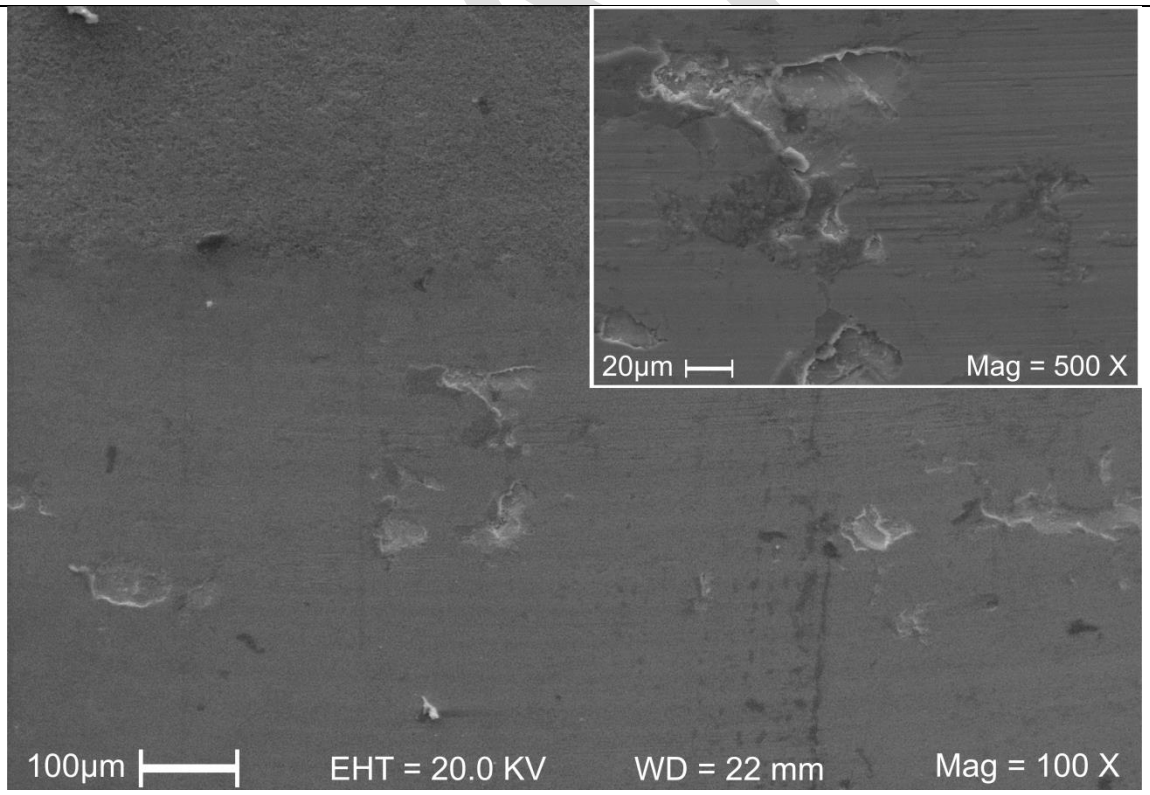

(b) +500 mV_{SCE}

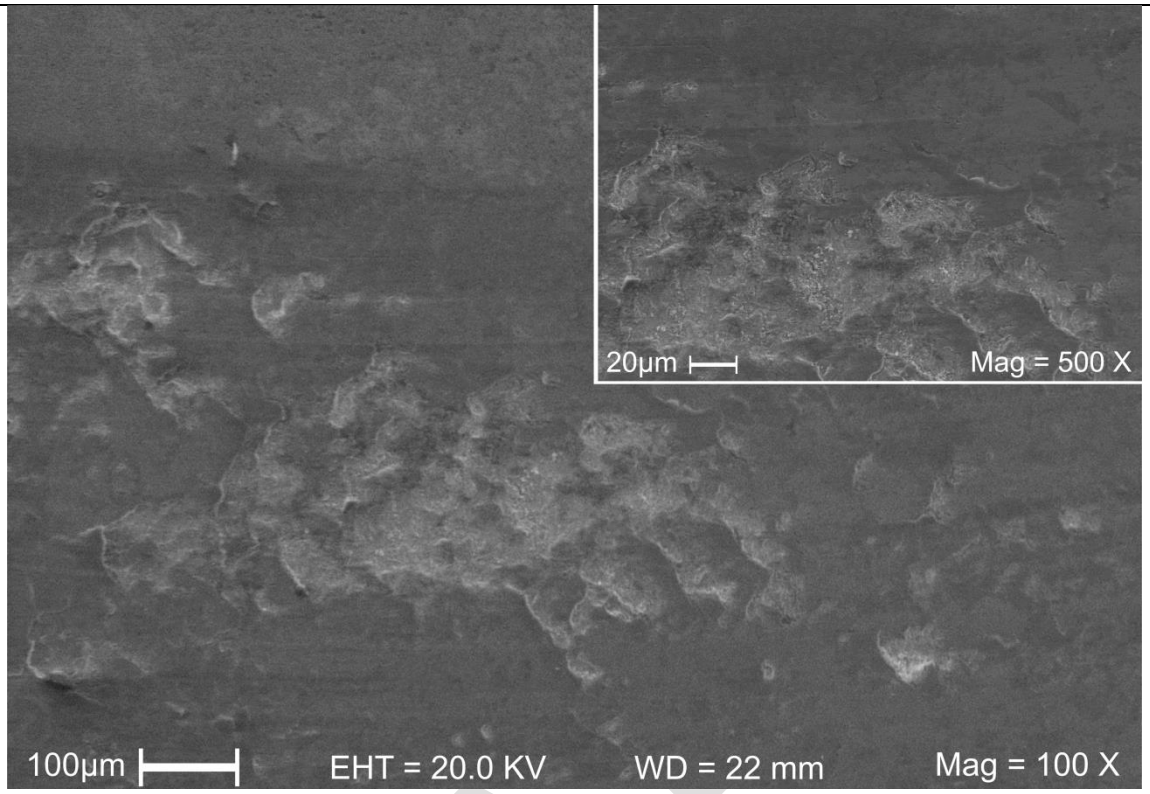

(c) OCP

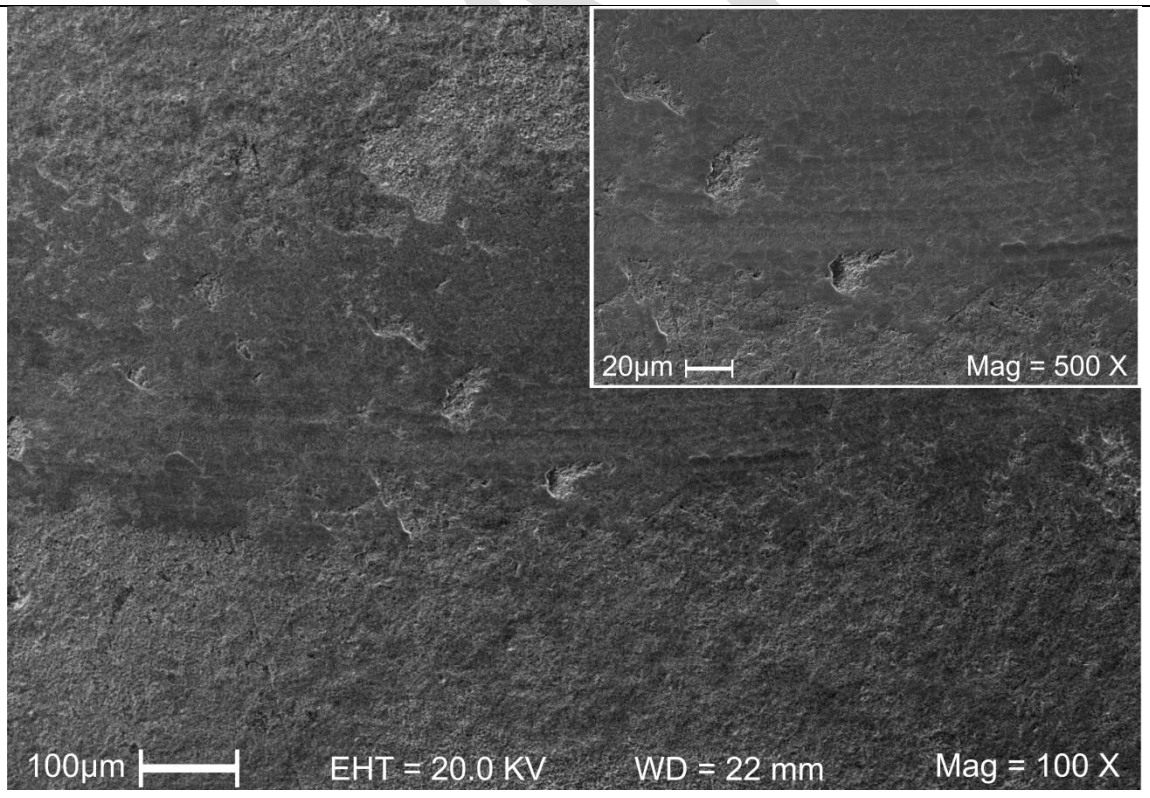

(d) -900 mV_{SCE}

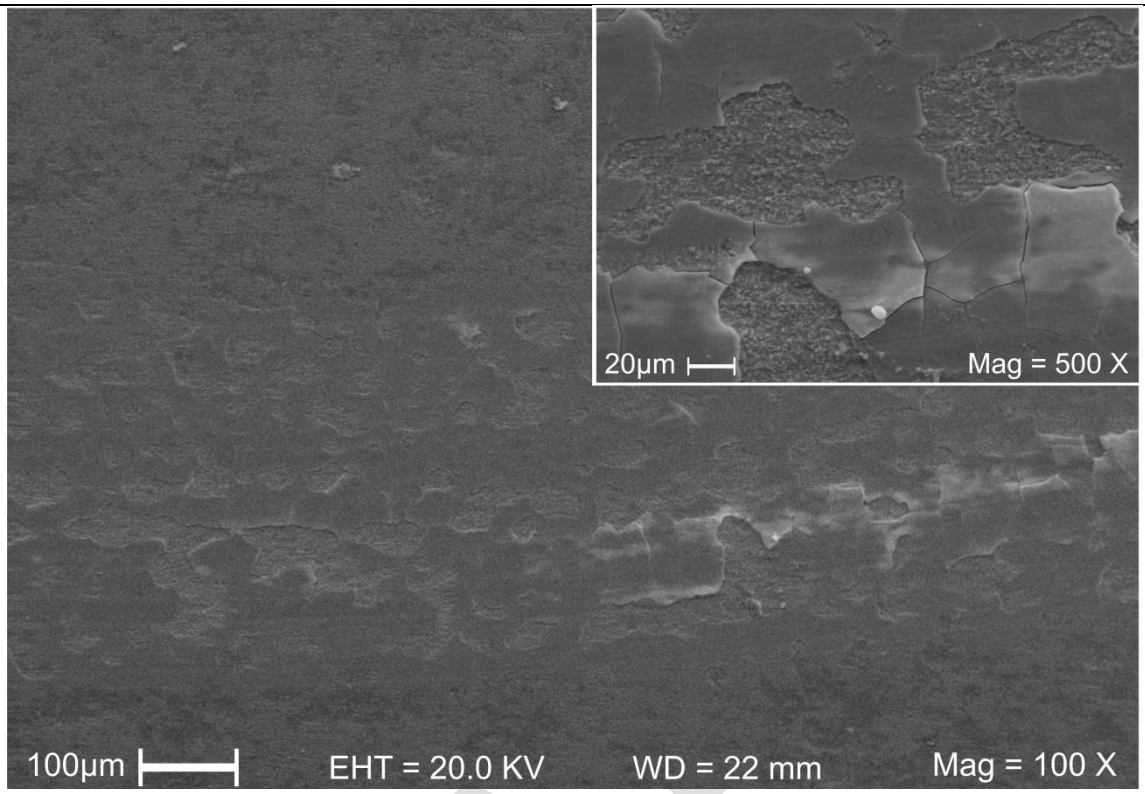

(e) -1500 mV_{SCE}

Fig.6: SEM images showing the wear track morphology produced on the PCOD-Ti, after tribocorrosion testing at potentials of: a) 1000 mV_{SCE}, b) 500 mV_{SCE}, c) OCP, d)-900 mV_{SCE} and e) -1500 mV_{SCE}. All tests were conducted using a load of 20 N for 10800 s.

3.3. Total material loss rate

Using a stylus profilometer the total material loss (TML) from the wear track was measured, this was then normalised with the sliding distance and applied load. This generates a value known as the total material loss rate (TMLR). The results are shown in Fig.12 as a function of applied potential for the PCOD-Ti and untreated CP-Ti samples.

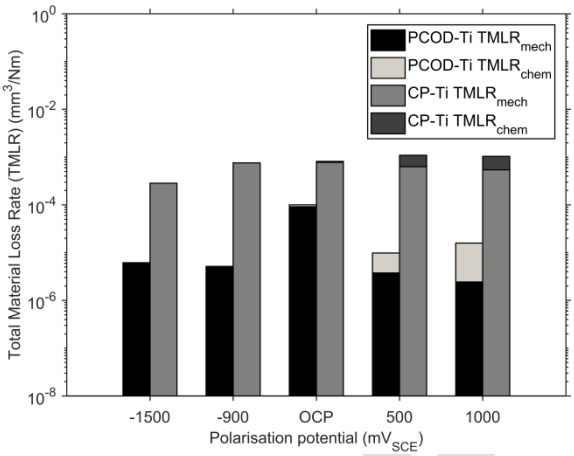

Fig. 12: Contribution of mechanical wear and corrosion to total material loss rate volume of pack carburised titanium and untreated titanium. All tests were conducted in a 0.9 % NaCl solution.

The chemical contribution of wear was determined using the currents measured during anodic polarisation via Faraday's law (Eq.4). Where I is the average current, t is time, F is faraday's constant, M is the atomic mass, n is valence and ρ is density.

$$V_{chem} = \frac{ItM}{nF\rho} \quad (4)$$

In order to calculate the amount of material lost to corrosion at OCP, both [37] and [38] used the Buller Volmer equation to calculate anodic current passing through the wear track (i_a). Once the current has been calculated Faraday's law can then be used to calculate the volume lost due to the chemical interaction (V_{chem}). The Buller Volmer equation takes into account the cathodic kinetics and the corrosion potential of the alloy, the potential present during sliding contact and the anode to cathode area ratio. From this model, the anodic current passing through the wear track (i_a) was calculated using Eq.5.

$$\log I_a = \frac{E_{corr} - E_c + a_c}{b_c} - \log\left(\frac{A_a}{A_c}\right) \quad (5)$$

where E_c is the potential measured during rubbing (OCP sliding Fig.10, E_{corr} is the corrosion potential (-204 mV from Fig.7), a_c and b_c are the Tafel constants extracted from the cathodic polarization curves (a_c = -825 mV, b_c = 274 from Fig.7). A_a corresponds to the wear track area after sliding (0.3 cm^2), A_c corresponds to the cathode area which can be approximated by the sample area (1.23 cm^2).

Fig.12 clearly demonstrates the effective wear reducing properties of the PCOD treatment, when compared with that of CP-Ti. The treatment reduced the TMLR across the spectrum by at least one order of magnitude.

The effect of potential on the tribocorrosion properties of titanium is as expected, and follows that of a valve metal. When subjected to anodic potentials the contribution of corrosion on the TMLR is increased. However, when charged cathodically initially the chemical wear is all together removed. When at extreme cathodic potentials, hydrogen embitterment occurs which seems to have the effect of reducing the TMLR of untreated titanium.

When evaluating the effect of potential on the tribocorrosion performance of PCOD-Ti, it is clear to see that potential has a dramatic effect on the TMLR recorded. When anodic potentials of +500 mV_{SCE} and +1000 mV_{SCE} are applied the TMLR is much reduced over that of the samples tested at OCP. However, the amount of wear attributed to corrosion (V_{chem}) is dramatically increased as indicated by the larger currents developed during sliding (Fig.11). It is believed that when anodically polarised the decomposition of TiC to TiO_2 (Eq.3) is greatly increased, resulting in the formation of a TiO_2 barrier film. TiO_2 has good tribological properties and helps to keep mechanical wear to a minimum. During the course of the test the TiO_2 film will be removed and as a result more TiC will be converted to TiO_2 thus generating the anodic currents, low friction and the low TMLR.

When the PCOD-Ti was tested under cathodic potentials of -900 mV_{SCE} and -1500 mV_{SCE} there was a much reduced TMLR recorded. This increased reduction is more than simply the removal of the anodic current/corrosion. At such cathodic potentials the hydrolysis of water is predicted. The solubility of H in Ti results in the formation of titanium hydride (Fig.8). The formation of titanium hydride has been shown to decrease the rate of material loss under tribocorrosive conditions for both oxidised and untreated titanium [16]. When polarised to -900 mV_{SCE} there will be less hydrogen embitterment than that of the sample polarised to -1500 mV_{SCE}. This will result in slightly less cracking and de-lamination of the hard hydride film, this is clearly observable in the SEM wear track images in Fig.11 and is accountable for the change in TMLR between the two voltages.

4. Conclusions

1. Pack carburization with limited oxygen diffusion produced a carbon rich subsurface network atop an extended oxygen diffusion zone.
2. The pack carburizing with limited oxygen diffusion has a limited impact on the corrosion resistance of titanium. Carburization resulted in an anodic shift in OCP, this suggests, it will initially be less likely to corrode. However, when polarized anodically higher current densities were observed than those recorded for untreated titanium.
3. During tribocorrosion testing conducted at OCP, three distinct frictional zones can be observed: Zone 1 is described as the interaction between the alumina and the TiC film. Zone II is the partial removal and gradual breakdown of the film within the wear track and zone III is the exposure and sliding contact between the alumina ball and the oxygen diffusion zone.
4. When anodically charged to 1000 mV_{SCE} and 500 mV_{SCE} the samples showed improved wear resistance over the sample tested under open circuit conditions. The hydrolysis of water and the formation of TiO_2 are increased at the surface, acting as a barrier providing low friction and wear.
5. At cathodic potentials of -1500 mV_{SCE} the formation of titanium hydride created a hardened zone within the wear track. This reduced the rate of wear, but also increased the Coefficient of friction.

Acknowledgement

One of the authors (RB) would like to acknowledge the financial support of De Montfort University for providing a PhD scholarship. Special thanks are also due to The Alderman Newton's Educational Foundation, The Sidney Perry Foundation and The Wyvernian Foundation for providing additional financial support during the course of this work.

References

Conflict of interest

On behalf of all authors, the corresponding author states there is no conflict of interest.